Current Biology, Vol. 13, 1423–1428, August 19, 2003, ©2003 Elsevier Science Ltd. All rights reserved. DOI 10.1016/S0960-9822(03)00547-5

The Minus End-Directed Motor Kar3 Is Required for Coupling Dynamic Microtubule Plus Ends to the Cortical Shmoo Tip in Budding Yeast

Paul S. Maddox, Jennifer K. Stemple, Lisa Satterwhite, E.D. Salmon, and Kerry Bloom*
Department of Biology
University of North Carolina, Chapel Hill
Chapel Hill, North Carolina 27599-3280

Summary

The budding yeast shmoo tip is a model system for analyzing mechanisms coupling force production to microtubule plus-end polymerization/depolymerization. Dynamic plus ends of astral microtubules interact with the shmoo tip in mating yeast cells, positioning nuclei for karyogamy [1]. We have used live-cell imaging of GFP fusions to identify proteins that couple dynamic microtubule plus ends to the shmoo tip. We find that Kar3p, a minus end-directed kinesin motor protein, is required, whereas the other cytoplasmic motors, dynein and the kinesins Kip2p and Kip3p, are not. In the absence of Kar3p, attached microtubule plus ends released from the shmoo tip when they switched to depolymerization. Furthermore, microtubules in cells expressing *kar3-1*, a mutant that results in rigor binding to microtubules [2], were stabilized specifically at shmoo tips. Imaging of Kar3p-GFP during mating revealed that fluorescence at the shmoo tip increased during periods of microtubule depolymerization. These data are the first to localize the activity of a minus end-directed kinesin at the plus ends of microtubules. We propose a model in which Kar3p couples depolymerizing microtubule plus ends to the cell cortex and the Bim1p-Kar9p protein complex maintains attachment during microtubule polymerization. In support of this model, analysis of Bim1p-GFP at the shmoo tip results in a localization pattern complementary to that of Kar3p-GFP.

Results and Discussion

Astral microtubule plus ends are coupled to the cell cortex at the shmoo tip of *S. cerevisiae* during both polymerization and depolymerization [1]. Previous studies identified the cortical protein Kar9p together with the microtubule binding protein Bim1p [3, 4, 5, 6, 7] as being important for microtubule attachment to the shmoo tip. Bim1p (like its mammalian homolog, EB1) preferentially binds polymerizing and not depolymerizing microtubule plus ends [8, 9]. Therefore, other proteins probably couple depolymerizing microtubule plus ends to the cell cortex. To test if microtubule motor proteins couple dynamic microtubule plus ends to the shmoo tip, we assayed shmoo tip microtubule dynamic attachment in cells lacking each of the cytoplasmic microtubule motor proteins. Wild-type or mutant cells expressing GFP-Tubulin (GFP-Tub1p, Experimental Procedures) were either treated with α-factor or mixed with wild-type α cells to induce shmoo formation. Astral microtubule dynamics relative to the shmoo tip were recorded by time-lapse digital microscopy (Experimental Procedures). Because astral microtubules polymerize and depolymerize from their plus ends only, movement of the spindle pole body (SPB) relative to the shmoo tip was indicative of the polymerization state of shmoo tip microtubule plus ends [1, 10]. When the SPB moved away from the shmoo tip, the microtubule plus ends were polymerizing, and upon microtubule shortening the SPB moved toward the shmoo tip [1].

The plus end-directed kinesins Kip2p and Kip3p as well as dynein contribute to astral microtubule-dependent nuclear orientation during the vegetative cell cycle [11]. However, neither *kip3*Δ, *kip2*Δ, nor *dynein*Δ affected microtubule attachment to the shmoo tip (Table 1). Furthermore, shmoo tip microtubules displayed normal dynamics (Table 1) in cells lacking Kip2p, Kip3p, or Dhc1p. Therefore, these cytoplasmic microtubule motor proteins important for nuclear orientation in mitosis are not required for microtubule dynamics at the shmoo tip.

In contrast, deletion of the minus end directed-kinesin Kar3p resulted in defective astral microtubule attachment to the shmoo tip. Kar3p was identified in a genetic screen for karyogamy mutants, and it was proposed that it physically pulls two haploid nuclei together on anti-parallel cytoplasmic microtubules [2]. *kar3* null cells responded to α factor by exhibiting G1 arrest and polarized cell wall growth that formed a shmoo. The dynamic properties of cytoplasmic microtubules located in the cell body were indistinguishable from those of wild-type cells (Table 1). However, time-lapse analysis of microtubule dynamic attachment to the shmoo tip revealed a clear defect (Figure 1A; supplemental Movie 1, available with this article online). Specifically, microtubules detached from the shmoo tip cortex when they switched to depolymerization (catastrophe; Figure 1A, closed arrows). After catastrophe, 66% of the microtubules lost attachment to the shmoo tip (as opposed to 2% in wild-type; more than 300 min of data for each, 15 cells). Because microtubule depolymerization occurs only at plus ends [1, 10], these results indicate that Kar3p is required for coupling depolymerizing microtubule plus ends to the shmoo tip cortex.

To investigate the mechanistic role of Kar3p, we used the dominant mutant *kar3-1*, which contains a single amino acid substitution (Gly 479 to Glu) located in the conserved ATP binding/hydrolysis site [2]. Similar mutations in other motor proteins cause rigor binding to microtubules [12]. Microtubule plus ends localize to shmoo tips in *kar3-1* cells (Figure 1B, arrowhead; supplemental Movie 2); however, these shmoo tip microtubules were not dynamic. In *kar3-1* cells, shmoo tip microtubules were paused (less than 0.1 μm/min growth or shortening rate) 80% of the time, whereas shmoo tip microtubules in wild-type cells rarely paused (5% of the time, Figure 1C). The average length of shmoo tip microtubules was

*Correspondence: kbloom@email.unc.edu

Table 1. Quantification of Microtubule Plus End Dynamic Attachment to the Shmoo Tip

		Shmoo Tip	Shmoo Tip	Cell Body	Cell Body
	MT Attach to Shmoo Tip	MT Polymerization Rate (Average Duration in Minutes)	MT Depolymerization Rate (Average Duration in Minutes)	MT Polymerization Rate (Average Duration in Minutes)	MT Depolymerization Rate (Average Duration in Minutes)
WT	99%	0.5 ± 0.3 μm/min (2.4)	0.5 ± 0.4 μm/min (2.3)	1.0 ± 0.6 μm/min (1.8)	0.9 ± 0.6 μm/min (1.6)
kar9	10%	NA	NA	1.2 ± 0.4 μm/min (1.9)	1.5 ± 0.6 μm/min (1.5)
bim1	35%	NA	NA	1.0 ± 0.4 μm/min (1.9)	1.4 ± 0.7 μm/min (1.7)
kar3	60%	NA	NA	0.7 ± 0.5 μm/min (2.1)	1.0 ± 0.3 μm/min (1.9)
kar3-1	96%	NA	NA	0.8 ± 0.4 μm/min (2.0)	0.9 ± 0.4 μm/min (1.9)
kip2	95%	0.6 ± 0.5 μm/min (2.5)	0.9 ± 0.6 μm/min (2.1)	0.7 ± 0.5 μm/min (2.2)	1.3 ± 0.6 μm/min (1.7)
kip3	89%	0.5 ± 0.5 μm/min (2.5)	0.8 ± 0.5 μm/min (2.0)	1.2 ± 0.5 μm/min (1.8)	1.6 ± 0.8 μm/min (1.6)
dhc1	96%	0.5 ± 0.4 μm/min (2.6)	0.9 ± 0.5 μm/min (2.0)	0.9 ± 0.5 μm/min (2.0)	0.7 ± 0.6 μm/min (2.2)

Comparison of dynamic properties of microtubules attached to the shmoo or free ends in wild-type and mutant strains. Percentages were calculated from observation of cell populations (three experiments, n = 100 each) and notation of the presence or absence of at least one microtubule plus end interacting directly with the shmoo tip cell cortex. Rate values are averages ± standard deviation of at least 25 measurements for each condition.

similar in *kar3-1* (1.75 μm) and wild-type cells (1.96 μm). Free astral microtubules in the cell body exhibited polymerization and depolymerization rates similar to those of the wild-type (0.79 ± 0.4 μm/min, n = 30 and 0.9 ± 0.4 μm/min, n = 27 in *kar3-1*; and 1.0 ± 0.6 μm/min, n = 40 and 0.8 ± 0.4 μm/min, n = 33 in the wild-type, respectively). Therefore, *kar3-1* specifically stabilized microtubules at the shmoo tip, suggesting that the ATPase activity of Kar3p is critical for microtubule plus end dynamics at the shmoo tip.

To determine the site of Kar3p function, we coimaged Kar3p-GFP with a SPB fluorescent marker (Spc29p-RFP [13]; Figure 2A; supplemental Movie 3). Kar3p-GFP was seen to bind the shmoo tip as well as the SPB and was seen to bind diffusely along shmoo tip microtubules. Interestingly, Kar3p-GFP intensity at the shmoo tip increased as the SPB moved toward the shmoo tip (microtubule plus end depolymerization, Figure 2B). During microtubule plus end polymerization, Kar3p-GFP decreased at the shmoo tip, where it diminished to undetectable levels in 70% of the cases. These results indicate that Kar3p localizes to the shmoo tip preferentially during microtubule depolymerization.

Kar3p is upregulated approximately 20-fold after exposure to α factor [2]. Exposure of cells to α factor resulted in localization of Kar3p-GFP to shmoo tip and non-shmoo tip microtubules. Figure 2C shows a cell expressing Kar3p-GFP treated with α-factor for approximately 3 hr. Note that a microtubule growing away from the shmoo tip has Kar3p-GFP signal. This localization is enhanced at microtubule plus ends (Figure 2C, arrow; supplemental Movie 4), indicating that Kar3p can act as a plus end binding protein. Kar3p's presence at microtubule plus ends at the shmoo tip is central to the persistence of a dynamic plus-end attachment. Furthermore, the finding that microtubules persist at shmoo tips in *kar3-1* mutants indicates that Kar3p's function to maintain dynamic attachment of plus ends depends on nucleotide hydrolysis.

The above results do not account for coupling microtubule plus ends to the shmoo tip during polymerization. Given that the vertebrate homolog of Bim1p (EB1) binds only to polymerizing microtubule plus ends both in vitro and in vivo [9, 14], we further investigated the role of Bim1p in coupling microtubule plus ends to the shmoo tip. Quantification of microtubule attachment to the shmoo tip in *bim1*Δ cells revealed that about 65% (157 out of 241) of the cells lacked shmoo tip attachment, whereas 35% of cells had microtubules at the shmoo tip (84 out of 241 total cells). In wild-type cells, nearly 100% had microtubules attached to the shmoo tip (247 out of 250 cells, Table 1). Thus, microtubule attachment to the shmoo tip was defective in *bim1*Δ mutants (Table 1 [3]). An enticing possibility is that Bim1p acts at the shmoo tip to maintain attachment to polymerizing microtubule plus ends when Kar3p is depleted and vice versa.

To investigate the interactions of Bim1p and microtubule attachment to the shmoo tip, we treated cells expressing Bim1p-GFP (C-terminal fusion to endogenous gene) with α-factor. Time-lapse sequences showed that Bim1p-GFP localized to several discrete spots in the cytoplasm (Figure 3; supplemental Movie 5). Punctate spots (0–3 at any given time point were observed) originating at the SPB moved linearly away from the SPB at rates of approximately 0.5 μm/min, similar to the rate of astral microtubule growth ([15]; see supplemental Movie 5). These spots probably mark the growing plus ends of microtubules and grew in all directions from the SPB, not only into the shmoo tip. Bim1p-GFP intensity was highly variable, and overall signal was lost rapidly as a result of photobleaching. However, analysis of Bim1p-GFP at the shmoo tip (Figure 3C) showed that the intensity of Bim1p-GFP increased (more than 2-fold in the example in 3C) while the SPB moved away from the shmoo tip. The Bim1p-GFP signal changed gradually; it increased continually during SPB movement away from the shmoo tip and then decreased during SPB movement toward the shmoo tip. This localization pattern is opposite to that observed for Kar3p. These results indicate that Bim1p-GFP localizes to the shmoo tip during times of microtubule polymerization and disperses upon depolymerization. Unlike Kar3p, Bim1p-GFP expressed at endogenous levels decorates all microtubule plus ends, including those that contact the cell cortex outside the shmoo region. However, the shmoo tip is the only site of microtubule plus-end attachment, indicating that some other component is required for recruiting or stabilizing Kar3p at the shmoo tip. This component is dependent upon microtubules because Kar3p's localization to the shmoo tip is lost upon treatment of cells

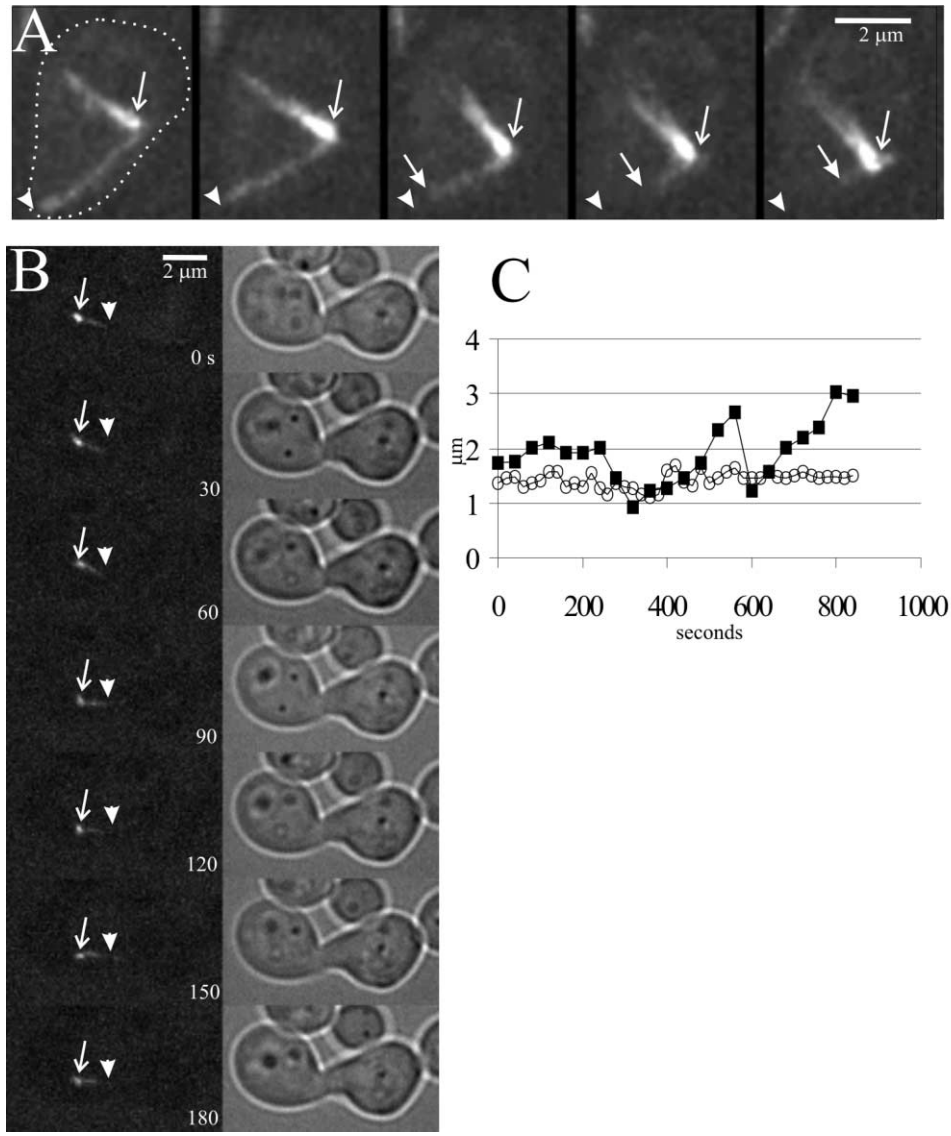

Figure 1. The Minus End-Directed Motor Protein Kar3p Is Required for Microtubule Attachment to the Shmoo Tip during Plus-End Depolymerization

(A) A cell expressing GFP-Tub1 and lacking Kar3p was treated with α factor for approximately 1.5 hr to induce shmooing (arrowhead). Time-lapse analysis of microtubules in this representative cell showed that microtubules interact with the shmoo tip in a limited fashion. Specifically, when a microtubule attached to the shmoo tip begins to depolymerize, attachment is lost and the microtubule (closed arrows) shortens toward the SPB (open arrows).

(B) Cells expressing the rigor binding mutant *kar3-1* are shown in a mating assay. The cell on the left is mutant, whereas the partner cell on the right is wild-type. Microtubules in the mutant cell attach to the cortex but fail to exhibit dynamics as seen by the lack of movement of the SPB (open arrows) relative to the shmoo tip (arrowheads).

(C) Analysis of this phenotype compared to wild-type is shown. Notice the attenuated dynamics of the mutant cell (open circles) compared to the wild-type (closed squares).

with nocodazole (data not shown). Interestingly, Kar9p is also localized to the shmoo tip in mating cells [11, 16]. Kar9p's localization during the vegetative cell cycle is regulated by phosphorylation (Cdc28-Clb5) and microtubule-based transport (Kip2) [17, 18]. It is likely that Kar3p transport and posttranslational modification contribute to its recruitment to the set of microtubules exclusively at the shmoo tip. The above results lead us to propose a model in which Bim1p and Kar3p are key regulators of microtubule plus-end dynamic attachment to the shmoo tip. In Figure 4 we envisage Bim1p, anchored to the cortex by Kar9p, maintaining attachment to growing microtubule plus ends at the shmoo tip. Kar3p (anchored to the cortex by an unknown factor) maintains the molecular interaction during microtubule plus-end shortening. In fact, the increased fluorescence of Kar3p on shortening microtubules leads to the hypothesis that Kar3p may promote persistent depolymerization and thereby prevents switching back to growth. This hypothesis is supported by the demonstration that

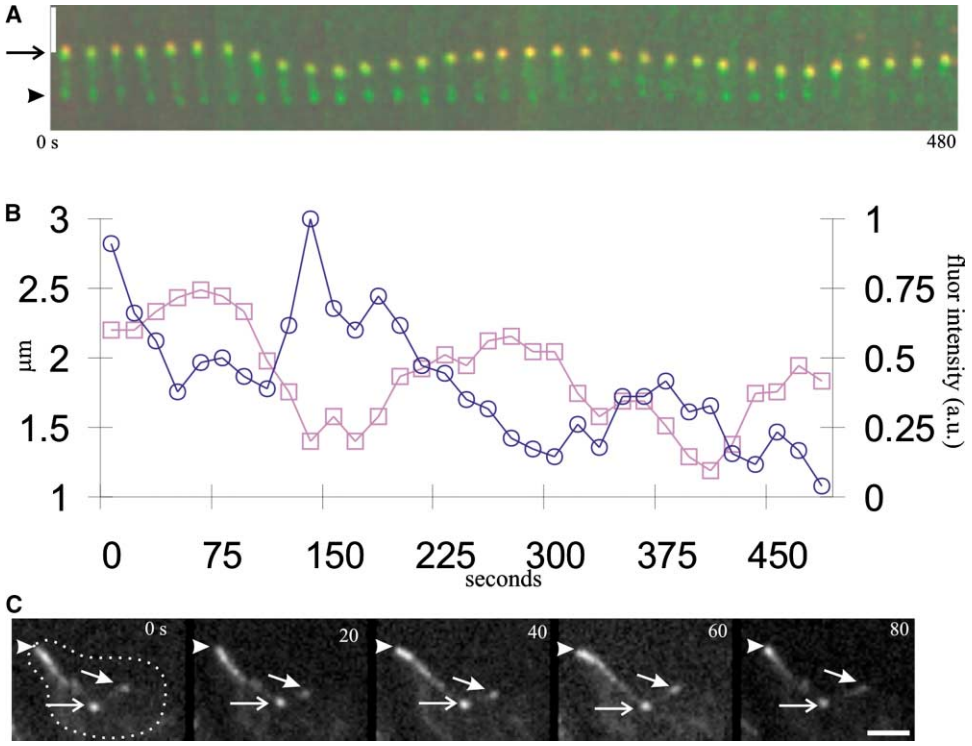

Figure 2. Kar3p-GFP Localizes to the Shmoo Tip Dynamically

(A) To observe Kar3p-GFP in a native situation, we used mating assays or brief treatments (approximately 1 hr) of α-factor. Also, to more accurately measure Kar3p-GFP relative to the spindle pole body, we coexpressed a red marker (Spc29p-dsRed) to label the SBP. Notice that when the spindle pole body (arrow) moves toward the shmoo tip (microtubule depolymerization) (arrowhead), Kar3p-GFP accumulates at the shmoo tip. The scale bar represents 2 μm.

(B) Quantification of Kar3p-GFP as a function of shmoo tip microtubule polymerization state shows that Kar3p-GFP (circles) accumulates approximately 2-fold during microtubule depolymerization when compared to periods of microtubule polymerization (squares; spindle pole body moving away from the shmoo tip).

(C) Five frames from a time lapse sequence showing a wild-type Kar3p-GFP-expressing cell treated with α-factor for approximately 2.5 hr to induce shmooing (arrowheads). Expression of Kar3p-GFP increases approximately 20-fold upon treatment with α-factor as described (Meluh and Rose, 1990) and localizes to microtubules outside of the shmoo tip (closed arrows) as well as to shmoo tip microtubules and the SPB (arrows). The scale bar represents 2 μm.

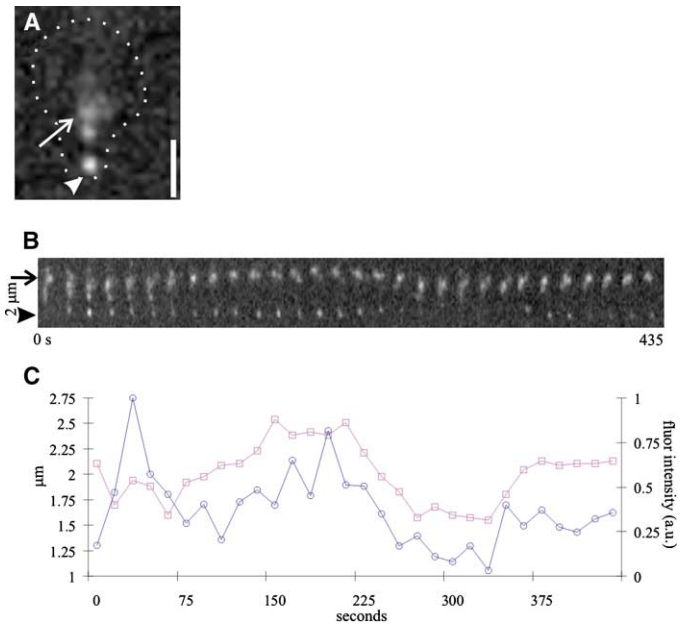

Figure 3. Bimp1-GFP Is More Intensely Localized to the Shmoo Tip during Microtubule Plus-End Growth

(A) A wild-type cell expressing Bim1p-GFP was treated with α-factor for approximately 1.5 hr to induce shmooing (arrowhead). The pattern of localization of Bim1p-GFP was a central SPB spot (open arrow) with smaller spots radiating outward. Analysis of GFP signal at the shmoo tip showed that Bim1p-GFP appeared and disappeared from the shmoo tip.

(B) Kymograph analysis shows that when the SPB (arrow) moved toward the shmoo tip (arrowhead), the GFP signal diminished.

(C) Graphical representation of Bim1p-GFP at the shmoo tip as a function of spindle pole body position. Further analysis of the intensity changes in Bim1p-GFP signal at the shmoo tip showed that when the spindle pole body moved away from the shmoo tip (microtubule polymerization at the shmoo tip), Bim1p-GFP increased on average 2-fold compared to times of microtubule polymerization. See text for details.

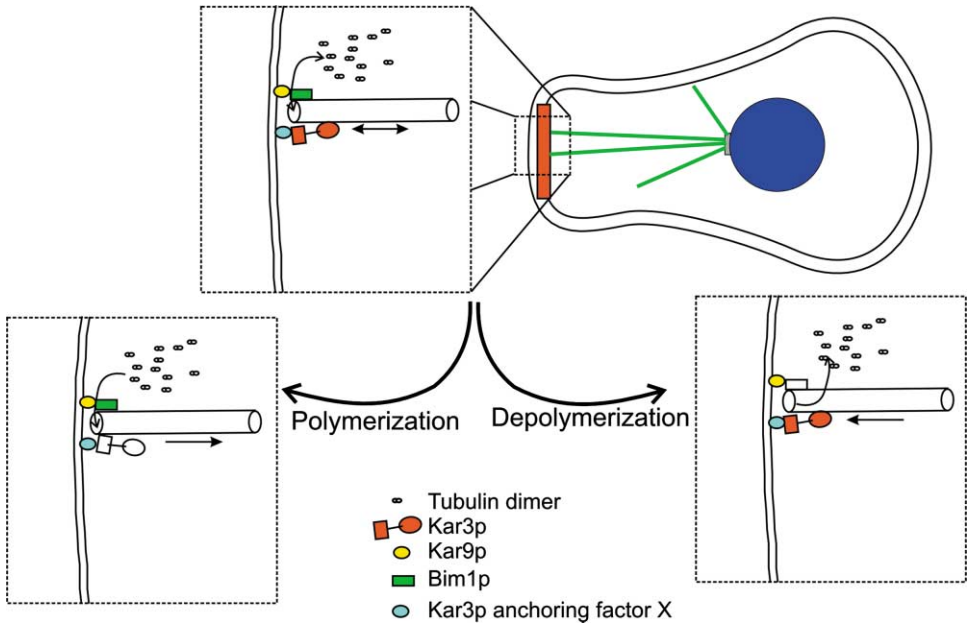

Figure 4. Model of the Mechanism of Microtubule Dynamic Attachment to the Shmoo Tip

Bim1p, anchored to the cortex by Kar9p, is present only during microtubule growth. Attachment to growing microtubule plus ends at the shmoo tip is mediated by Bim1p. Kar3p (anchored to the cortex by an unknown factor) is only present at shmoo tips during microtubule plus-end shortening. Kar3p acts to maintain the molecular interaction between shortening microtubule plus ends and the shmoo tip cell cortex.

plus end-directed kinesin-coated microspheres persistently bind shortening microtubule plus ends [19] and that microtubule depolymerization is enhanced under activating conditions for the kinesin motor [20]. The finding that disruption of the motor domain of Kar3p prevents microtubule dynamics but not attachment at the shmoo tip is consistent with the notion that Kar3p motor activity is required for tethering the shortening plus end to the shmoo tip. We propose that the key difference in microtubule plus-end attachment to the shmoo tip (mating) or the bud (vegetative) is the presence of Kar3p and, therefore, the ability to maintain attachment during microtubule depolymerization. This model should be relevant to studies of other microtubule dynamic attachment sites, such as kinetochores and the cortex of cells that undergo mitotic spindle rotation or asymmetric positioning.

Experimental Procedures

Cell Culture and Strain Construction

Cells were cultured with standard budding-yeast protocols. Knockout mutations were constructed by homologous recombination as described. Amino-terminal GFP labeling of TUB1 was a generous gift from Dr. Aaron Straight (Harvard Medical School) and has been described elsewhere. GFP fusion to BIM1 was constructed by carboxy-terminal genomic insertion, resulting in a single tagged copy of BIM1 under native promoter. We constructed GFP fusion to KAR3 by first knocking out endogenous KAR3 and then integrating the KAR3 promoter along with KAR3 fused to GFP at its carboxy terminus at the URA3 locus. The resulting KAR3-GFP fusion protein was expressed at endogenous levels.

Microscopy

Yeast were prepared for time-lapse imaging as described previously. Images were acquired either by spinning-disk confocal microscopy [21] or by wide-field multi-mode imaging [22]. Modifications to the wide-field imaging system in this study were limited. A full description of the imaging system is described elsewhere [23]. For all experiments here, the following conditions apply. Data were collected at room temperature (approximately 23°C) with a 100× 1.4 N.A. Plan Apo brightfield objective lens with camera binning set at 2 by 2. Through-focal series were collected at each time point during time-lapse acquisition, with a total of five focal positions spaced by 0.5 or 0.75 μm taken in fluorescence (GFP or GFP and RFP) and a single DIC or brightfield image taken at the mid-point of the focal series. Time-lapse intervals varied from 5 to 30 s depending on the experiment.

Analysis and Quantification

Analysis of microtubule growth and shortening rates was done by single-point tracking in MetaMorph software (UIC, Downingtown, PA). Through-focal series for each time point were projected by Maximum Projection for measurements in most cases. In some cases microtubules grow in the direction of the focus, and therefore three-deminsional analysis of microtubule growth was employed [24]. Microtubule lengths were recorded over the course of a time-lapse sequence and imported into Excel for quantification. Contrast enhancement was conducted in MetaMorph, and final figures were constructed in CorelDraw 10.

Supplemental Data

Five supplemental movies are available with this article online at http://www.current-biology.com/cgi/content/full/13/16/1423/DC1.

Acknowledgments

The authors would like to thank Arshad Desai, Amy S. Maddox, Chad Pearson, and Dale Beach for critical reading and helpful conversations regarding this manuscript. This work was supported in part by National Institutes of Health grants GM24364 and GM606780 to E.D.S. and GM32238 to K.B.

Received: April 24, 2003
Accepted: June 25, 2003
Published: August 19, 2003

References

1. Maddox, P., Chin, E., Mallavarapu, A., Yeh, E., Salmon, E.D., and Bloom, K. (1999). Microtubule dynamics from mating through the first zygotic division in the budding yeast Saccharomyces cerevisiae. J. Cell Biol. *144*, 977–987.
2. Meluh, P.B., and Rose, M.D. (1990). KAR3, a kinesin-related gene required for yeast nuclear fusion. Cell *60*, 1029–1041.
3. Schwartz, K., Richards, K., and Botstein, D. (1997). BIM1 encodes a microtubule-binding protein in yeast. Mol. Biol. Cell *8*, 2677–2691.
4. Miller, R.K., Heller, K.K., Frisen, L., Wallack, D.L., Loayza, D., Gammie, A.E., and Rose, M.D. (1998). The kinesin-related proteins, Kip2p and Kip3p, function differently in nuclear migration in yeast. Mol. Biol. Cell *9*, 2051–2068.
5. Korinek, W.S., Copeland, M.J., Chaudhuri, A., and Chant, J. (2000). Molecular linkage underlying microtubule orientation toward cortical sites in yeast. Science *287*, 2257–2259.
6. Lee, L., Tirnauer, J.S., Li, J., Schuyler, S.C., Liu, J.Y., and Pellman, D. (2000). Positioning of the mitotic spindle by a cortical-microtubule capture mechanism. Science *287*, 2260–2262.
7. Miller, R.K., Cheng, S.C., and Rose, M.D. (2000). Bim1p/Yeb1p mediates the Kar9p-dependent cortical attachment of cytoplasmic microtubules. Mol. Biol. Cell *11*, 2949–2959.
8. Tirnauer, J.S., O'Toole, E., Berrueta, L., Bierer, B.E., and Pellman, D. (1999). Yeast Bim1p promotes the G1-specific dynamics of microtubules. J. Cell Biol. *145*, 993–1007.
9. Tirnauer, J.S., Grego, S., Salmon, E.D., and Mitchison, T.J. (2002a). EB1-microtubule interactions in Xenopus egg extracts: role of EB1 in microtubule stabilization and mechanisms of targeting to microtubules. Mol. Biol. Cell *13*, 3614–3626.
10. Maddox, P.S., Bloom, K.S., and Salmon, E.D. (2000). The polarity and dynamics of microtubule assembly in the budding yeast Saccharomyces cerevisiae. Nat. Cell Biol. *2*, 36–41.
11. Miller, R.K., and Rose, M.D. (1998a). Kar9p is a novel cortical protein required for cytoplasmic microtubule orientation in yeast. J. Cell Biol. *140*, 377–390.
12. Nakata, T., and Hirokawa, N. (1995). Point mutation of adenosine triphosphate-binding motif generated rigor kinesin that selectively blocks anterograde lysosome membrane transport. J. Cell Biol. *131*, 1039–1053.
13. Elliott, S., Knop, M., Schlenstedt, G., and Schiebel, E. (1999). Spc29p is a component of the Spc110p subcomplex and is essential for spindle pole body duplication. Proc. Natl. Acad. Sci. USA *96*, 6205–6210.
14. Tirnauer, J.S., Canman, J.C., Salmon, E.D., and Mitchison, T.J. (2002b). EB1 Targets to kinetochores with attached, polymerizing microtubules. Mol. Biol. Cell *13*, 4308–4316.
15. Shaw, S.L., Yeh, E., Maddox, P., Salmon, E.D., and Bloom, K. (1997b). Astral microtubule dynamics in yeast: a microtubule-based searching mechanism for spindle orientation and nuclear migration into the bud. J. Cell Biol. *139*, 985–994.
16. Beach, D.L., Thibodeaux, J., Maddox, P., Yeh, E., and Bloom, K. (2000). The role of the proteins Kar9 and Myo2 in orienting the mitotic spindle of budding yeast. Curr. Biol. *10*, 1497–1506.
17. Liakopoulos, D., Kusch, J., Grava, S., Vogel, J., and Barral, Y. (2003). Asymmetric loading of Kar9 onto spindle poles and microtubules ensures proper spindle alignment. Cell *112*, 561–574.
18. Maekawa, H., Usui, T., Knop, M., and Schiebel, E. (2003). Yeast Cdk1 translocates to the plus end of cytoplasmic microtubules to regulate bud cortex interactions. EMBO J. *22*, 438–449.
19. Lombillo, V.A., Stewart, R.J., and McIntosh, J.R. (1995). Minus-end-directed motion of kinesin-coated microspheres driven by microtubule depolymerization. Nature *373*, 161–164.
20. Peskin, C.S., and Oster, G.F. (1995). Force production by depolymerizing microtubules: load-velocity curves and run-pause statistics. Biophys. J. *69*, 2268–2276.
21. Maddox, P.S., Moree, B., Canman, J.C., and Salmon, E.D. (2003). A spinning disk confocal microscope system for rapid high resolution, multimode, fluorescence speckle microscopy and GFP imaging in living cells. In Biophotonics, Parts A and B, Methods in Enyzmology, Vol. 360. G. Marriot and I. Parker, eds., (San Diego: Academic Press).
22. Salmon, E.D., Shaw, S.L., Waters, J., Waterman-Storer, C.M., Maddox, P.S., Yeh, E., and Bloom, K. 1998. A high-resolution multimode digital microscope system. In Methods in Cell Biology: Video Microscopy, Vol. 56, G. Sluder and D.E. Wolf, eds. (London: Academic Press).
23. Pearson, C.G., Maddox, P.S., Salmon, E.D., and Bloom, K. (2001). Budding yeast chromosome structure and dynamics during mitosis. J. Cell Biol. *152*, 1255–1266.
24. Shaw, S.L., Yeh, E., Bloom, K., and Salmon, E.D. (1997). Imaging green fluorescent protein fusion proteins in *Saccharomyces cerevisiae. Curr. Biol. 7*, 701–704.